ISTITUTO NAZIONALE DI FISICA NUCLEARE

Sezione di Genova

INFN/FM-93/01
9 Febbraio 1993

R. Vaccarone, M. Gaspari:

INTEGRANULAR FLUXONS IN HTSC

Servizio Documentazione
dei Laboratori Nazionali di Frascati

INFN – Istituto Nazionale di Fisica Nucleare
Sezione di Genova

INFN/FM–93/01
9 Febbraio 1993

INTERGRANULAR FLUXONS IN HTSC

R. Vaccarone and M. Gaspari †
I.N.F.N., Sezione di Genova
Via Dodecaneso 33, 16146 GENOA, ITALY

ABSTRACT

The low transport current in granular High T_c superconductors is undoubtely attributed to the presence of weak links between grains. Magnetization and critical current measurements at very low field indicates that this low transport current behaves as expected from a critical state model.

In this paper we examine the flux structures which can be present in such granular systems, at low magnetic fields, by using a two-dimensional model of the material, which is assumed to consist of S/C grains connected by weak links showing Josephson properties. We show that the discreteness of the the system is the cause of flux pinning and that by using very simple dinamical equations it is possible to study the critical state and the irreversible hysteresis which arouse in the sample under a varying magnetic field.

By using a very sensitive magnetometer based on a SQUID sensor we have detected the presence of the individual fluxons sitting in the samples and we have shown that even their movement in the sample can be detected.

1. Introduction.

Most of the High T_c superconductors are easily prepared in the form of granular aggregates by a sintering process. In such systems the grains have good superconducting properties and below some low critical field H_{c1} present a complete Meissner effect. The surface of separation between the grains is the weak point for the transport current, showing a critical current orders of magnitude lower than the grains. Anyway the material as a whole still shows superconducting properties. The junctions between the grains are superconducting weak links and show Josephson character, as nicely demonstrated in [1]. Save in the materials with very high density, a number of voids is left between the grains and these holes play an important role in determining the low field behaviour of these materials. The system can be indeed modeled as an array of SQUIDs, or as a network of Josephson junctions[2].

The system is truly tridimensional and with a very high disorder. We expect that in such a complex network nor the current can follow a regular straight path nor the field can be described by a two-dimensional map.

However in this paper we use simple two-dimensional regular models which will contain the fundamental physical features.

---

† In partial fullfillment of his thesis work

A linear array of Josephson junctions has been studied by Yamashita et al. [5] by means of a mechanical analog. Pinning has been detected but the critical state has not been searched. Networks of junctions in two dimensions have been studied by many authors [6,7], but all of them have neglected the effect of the self field and by this choice they where not able to obtain information about the existence of a critical state in the system.

2. Two-dimensional SQUID array.

A granular superconductor can be described by a two-dimensional array of superconducting grains connected by Josephson Junctions. We analize here a system with point-like junctions and with holes of a finite size (which of course can be well described as a SQUID array).

The grains are arranged at the corners of a square mesh and the junctions that connect adjacent grains are oriented along the coordinate axis.

We will label the grains by two indices i,j running respectively along the x and y axis; to any grain we can associate two junctions, starting from it and connecting it to the adjacent grain on the right, on x direction, or to the upper one, in the y direction; the unitary cell will contain also the hole on the right and above the i,j grain.

The equation wich describe the system can be written in terms of the phase difference across the junctions in x directions φ_x or in y direction φ_y. In the same way the current has two components I_x and I_y while the magnetic field b is directed along the z axis.

A static equation for the system can be obtained in the following way:

We consider a closed square path encircling an hole, with the four corners in the center of the grains i,j , $i+1,j$, $i+1,j+1$ and $i,j+1$, and crossing the junctions which connectes the four grains together. By integrating along this path the equation which relates the current density in the superconductor to the vector potential and the space variation of the phase of the wave function

$$j(r) = eh \left(\nabla\varphi - e/hcA(r)\right) {\psi_0}^2 \tag{1}$$

we obtain a relationship between the phase difference across the junctions and the flux enclosed in the hole.

$$\varphi_{x,i,j} + \varphi_{y,i+1,j} - \varphi_{x,i+1,j+1} - \varphi_{y,i,j} = 2\pi \frac{\Phi_{i,j}}{\Phi_0} \tag{2}$$

A second equation can be obtained by considering the field change on the two sides of the slab formed by subsequent junctions in the same direction (which in this model are infinite in the z direction)

$$\Delta_x b = \mu_0 \cdot I_x \tag{3a}$$

$$\Delta_y b = -\mu_0 \cdot I_y \tag{3b}$$

where I is the current in the junctions for unit lenght along z.

The junction current must be related to the phase difference according to the Josephson equation

$$I_x = I_{xm} \cdot \sin(\varphi_x) \tag{4a}$$

$$I_y = I_{ym} \cdot \sin(\varphi_y) \tag{4b}$$

From equations 2, 3, 4 we get the following system of difference equations:

$$\Delta_x(\Delta_x \varphi_y - \Delta_y \varphi_x) = \beta \cdot \sin(\varphi_y) \tag{5a}$$

$$\Delta_y(\Delta_x \varphi_y - \Delta_y \varphi_x) = -\beta \cdot \sin(\varphi_x) \tag{5b}$$

The field in the holes will be given by

$$b_{i,j} = \frac{\Phi_{i,j}}{S_{hole}} = \frac{\Phi_0}{S_{hole}} \cdot \frac{\varphi_{x,i,j} + \varphi_{y,i+1,j} - \varphi_{x,i+1,j+1} - \varphi_{y,i,j}}{2\pi} \tag{6}$$

and the grain size will enter only in determining the average field in a cell

$$\langle b \rangle_{i,j} = b_{i,j} \frac{S_{hole}}{(S_{hole} + S_{grain})} \tag{7}$$

The equations given above in particular cases can be put in the form of differential equations for a continuous medium, but in doing this we will loose the possibility to find pinning. Another important point must be given about the vector fields. While I_s has null divergence in the continuous limit, the same is not true for φ_s.

The difference equation 5 can be solved with suitable boundary conditions and a solution representing a single fluxon can be found. If a square region of the lattice of sufficient size is considered, the solution will hardly depent on the boundary conditions, and the fluxon can be taken as insulated. We will describe now the caracteristics of such an object. The field profile in the holes of the lattice is shown in fig. 1.

We can define the size of the fluxon as the radius of the circle which contains half a flux quantum. We call this lenght Λ_Φ which is found to be almost exactly

$$\Lambda_\Phi = \frac{\pi}{\sqrt{\beta}} = \pi \cdot \lambda_j \tag{8}$$

The current density decays at large radii (where an average over many junctions in azimutal direction is meaningful) as

$$\langle j \rangle \propto K_1(r\sqrt{\beta}) \tag{9}$$

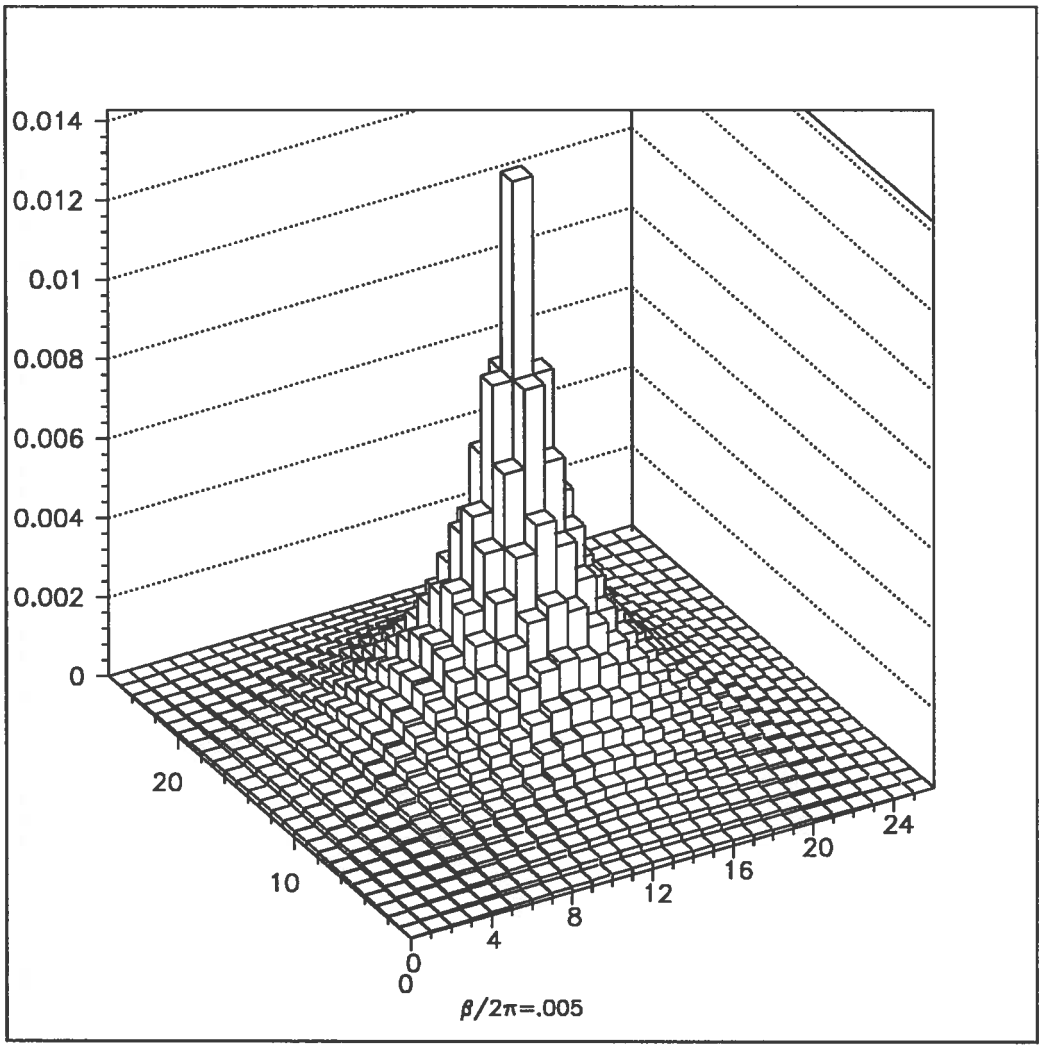

Figure 1: A lego plot of the field profile for a single fluxon in a square mesh of 26 × 26 cells.

and the average field behaves as

$$\langle b \rangle \propto K_0(r\sqrt{\beta}) \tag{10}$$

At large radii the current density has rotational simmetry around the fluxon center. The current density attains is maximum at the junctions enclosing the central hole, irrespective of the magnitude of the parameter β.

3. Fluxon pinning and interaction.

The normalized energy density in the array can be calculated easily by adding together the magnetic term ε_m due to the field in the holes and the term ε_J due to the current flowing in the junctions

$$\varepsilon_{i,j} = \varepsilon_{m\,i,j} + \varepsilon_{J\,i,j} = {b_{i,j}}^2/2 + (1 - cos(\varphi_{x\,i,j})) + (1 - cos(\varphi_{y\,i,j})) \tag{11}$$

The energy of an insulated fluxon is obtained by summing over the cells of the whole mesh the energy density.

In our reduced units the self energy varies with λ_j as $1/\lambda_j^2$.

As in the onedimensional case[4,8] we can consider the state with the fluxon centered in the hole or over a junction (i.e. shared between two adjacent holes). The fluxon energy will be different in the two cases and this difference gives the energy barrier to overcame in moving across the junctions network. The barrier energy as a function of β is given in fig. 2. Because periodic boundary conditions are used, the network size gives also the fluxon spacing.

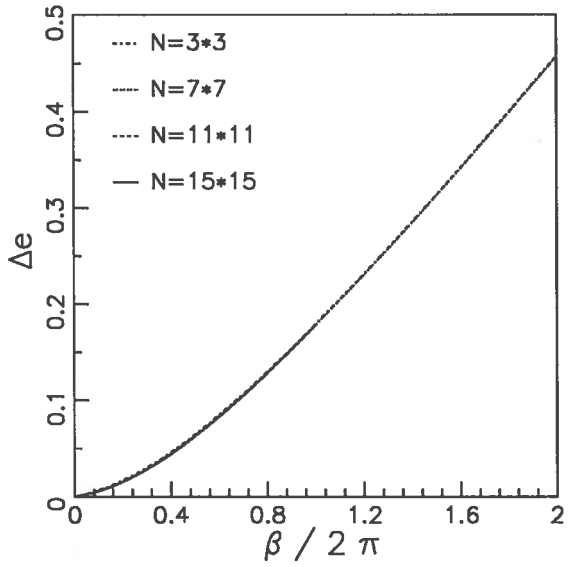

Figure 2: The pinning energy as a function of β for an insulated fluxon in a network of SQUIDs.

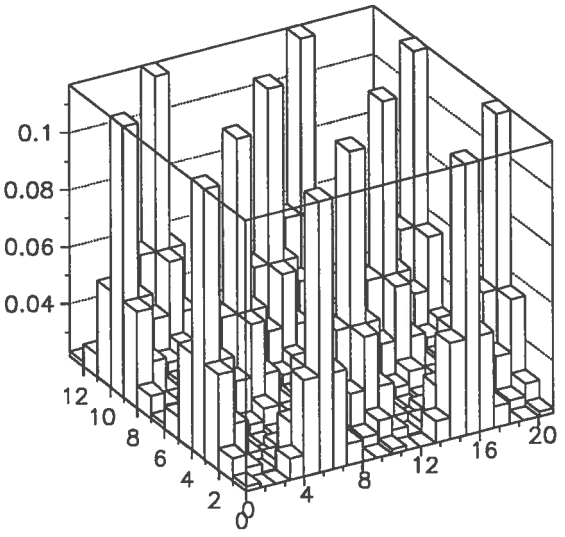

Figure 3: An example of a triangular fluxon array used to find the interaction energy. The elementary cell is 10 × 6 mesh sites.

The fluxon interaction reveals itself by an increase in the fluxon energy, which depends on the fluxons size and their distance T_{ff}.

To study the interaction force we have considered simple fluxon arrays forming a square or a triangular mesh.

The interaction energy depends on λ_j / T_{ff} with a quadratic law being valid when $\lambda_j \gg 1$ and the spacing is greater than $2\lambda_j$.

In conclusion we can see the fluxon as a particle with self energy (rest mass), sitting in a periodic potential, and interacting with other fluxons.

4. The dinamical equation and the magnetization cycles.

From the system of difference equation wich describe our SQUID array it is possible to obtain field profiles with a gradient which is linear on the average, but shows even the individual fluxons sitting in the sample.

The use of a dinamical equation allows us to verify that the system behaves according to the critical state model, and to obtain magnetization cycles or $VvsI$ plots.

In two dimensions the discrete Sine-Gordon equations, with a dissipative term representing the normal conductivity of the weak links are:

$$\Delta_x(\Delta_x \varphi_y - \Delta_y \varphi_x) = \gamma \frac{\partial^2 \varphi_y}{\partial t^2} + \beta \cdot \sin(\varphi_y) + \eta \frac{\partial \varphi_y}{\partial t} \qquad (12a)$$

$$\Delta_y(\Delta_x \varphi_y - \Delta_y \varphi_x) = \gamma \frac{\partial^2 \varphi_x}{\partial t^2} - \beta \cdot \sin(\varphi_x) + \eta \frac{\partial \varphi_x}{\partial t} \qquad (12b)$$

The coefficients γ , β and η are given by:

$$\gamma = \mu_0 C S_{hole} \qquad (13a)$$

$$\beta = \frac{2\pi \mu_0 S_{hole} I_m}{\Phi_0} \qquad (13b)$$

$$\eta = \frac{\mu_0 S_{hole}}{R} \qquad (13c)$$

where C and R are the junction capacitance and shunt resistance and I_m is the maximum Josephson current; S_{hole} is the hole area and $\mu_0 S_{hole}$ is equivalent to the self inductance of the loop encircling the hole. Both I_m, C, R and L are calculated per unit length along the field direction.

We obtain a resistance $R = 10^{-5}\Omega/m$, starting from a typical resistivity of $1\, m\Omega\, cm$. The capacitance C is about 1. 10^{-8} F for an oxide barrier 50 $\AA$ thick, but can be orders of magnitude lower for S-N-S junctions. If we consider a square mesh of grains and we impose as boundary conditions an external field changing in time on the peripheral cells, the field in the sample evolve according to a critical state model, and the total flux linked with the square domain shows a typical hysteresis cycle. In the present simulation we have neglected the finite size of the junctions and the magnetization is expected to follow the Bean model[3]. A magnetization cycle obtained for a square mesh of 14 $\times$ 14 cells at $\beta/2 \cdot \pi = 1.3$, with high damping and zero junction capacitance ($\eta = 1$, $\gamma = 0$) is shown in Fig. 4. The external field H_{ext} is normalized to the field which gives a flux quantum in an hole (of unit area). The magnetic field profile has a slope near one and the sample is almost fully penetrated. The cycle has an overall shape which agrees with the Bean model with large steps superimposed on it. At any step a large number of fluxons enter in the sample or leave it. Indeed at high βs on the surface of the sample we find a onedimensional flux profile, from which single fluxons enucleates, moving inside where a truly two-dimensional arrangment is present. Another example is given in Fig. 5. The $\beta/2\pi$ value is lower than unit and the fluxons will have a larger size and larger separation.

This graph shows first of all that even at low β the pinning exists and the critical state is in effect. The shape of the curve cannot be compared with a Bean

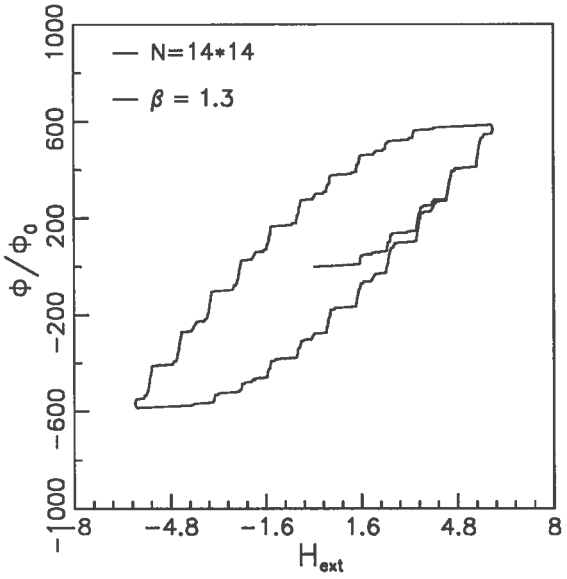

Figure 4: The hysteresis cycle obtained in a SQUID network with high pinning ($\beta = 1.3$).

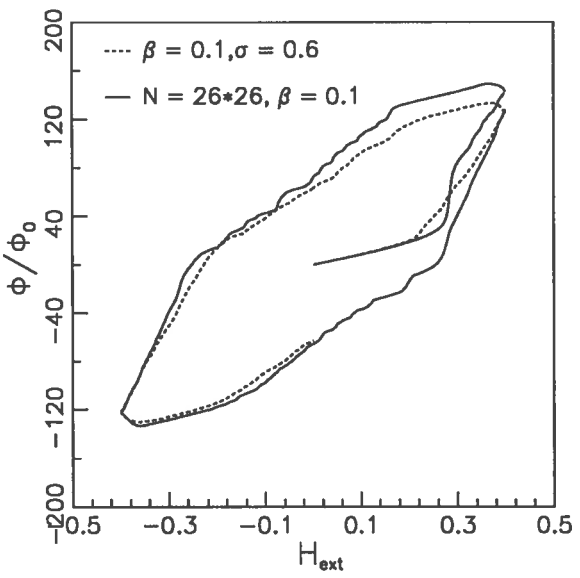

Figure 5: A system with low pinning and uniform (continuous line) or statistically distributed (dashed line) junction currents.

cycle, because single fluxon effects are important. In this case the steps due to surface shielding are reduced and the movement of the flux profile in the bulk can be seen better.

The results for a SQUID network with Junction currents distributed statistically with a variance of 0.6 are shown on the same graph. The main point we want to stress is that the cycle amplitude, i.e. the critical current in the system, is almost unchanged. Indeed a granular system has pinning due to the presence of voids even in absence of any statistical distribution of its properties.

5. The magnetometer

A simple SQUID magnetometer has been built to measure the magnetization of small samples of granular High T_c Superconductor in the low field range where single fluxon effects are expected to show up.

The magnetometer is designed to allow fast recording of magnetization cycles in magnetic fields ranging from 0.1 μT to a few mT on samples with a minimum section area of 10^{-9} m^2. At the actual stage the measurements can be performed at a fixed temperature of 4.2 K.

The magnetometer is housed in a glass dewar, and both the SQUID probe, the coil assembly and the sample are immersed in liquid He. Liquid Nitrogen surrounds the Helium criostat and a Mumetal shield at room temperature is used to reduce the external fields to about 3 μT.

The flux measuring devices is a commercial SQUID detector (BTi 330X

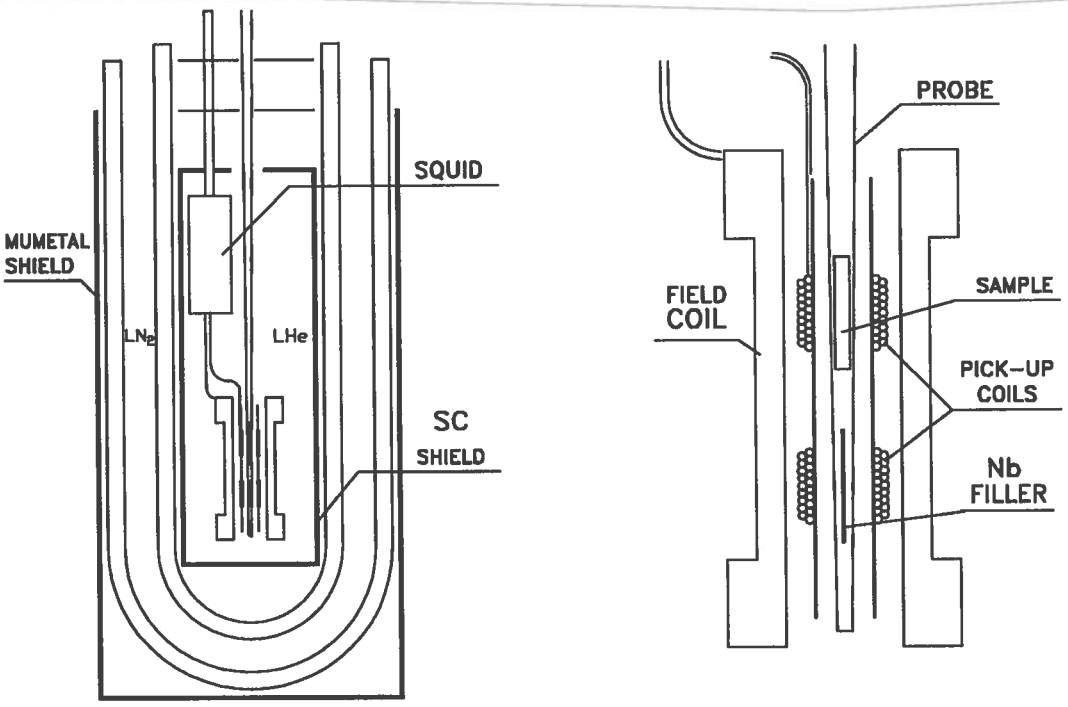

Figure 6: Schematic view of the magnetomether: general view (left), expanded view of the magnetic field coil, gradiometer and sample area (right).

Series SQUID measurement system with HYBRID SQUID sensor and MFP probe) coupled to the sample by a superconducting flux transformer. Two pick-up coils wound in opposite directions are used, to form a first order gradiometer. The coils are made with NbTi wire, in two layers of 13 turns each, on a fiberglass coil former of 3.9 mm diameter. The center to center distance of the coils is 16 mm. The transformer as a flux transfer ratio of 1 / 14.

The field coils is 60 mm long with an inner diameter of 7 mm. The winding is made with copper wire, 32660 turn/m, with correction coils 4.5 mm long at the ends.

The experimental area is surrounded by a Superconducting Lead shield.

A general view of the cryostat is given in Fig. 6 (left). On the right we show an expanded view of the detection assembly. It is possible to see the two opposite pick-up coils containing the sample and a few short wires of Nb which are used for a first order compensation of the gradiometer umbalance. The use of such a filling allows us to get compensation of the flux transformer at $\sim 1/3000$ starting from the as-done astatic coils with an umbalanced flux of $\sim 1/200$.

6. Magnetometer operation

With this magnetometer it is possible to obtain magnetization cycles in a fast and straightforward way.

The samples can be changed at any time by inserting them in a top-loading probe. During cool down the sample reaches its transition temperature in a low field zone, inside the Mumetal shield.

The sample is then exposed to a triangular periodic magnetic field (usually 6 to 18 cycles of the same amplitude) generated by a digital source of high accuracy and low noise. A cycle is completed in two and a half minutes.

The magnetic flux is recorded (1000 points per cycle) and an averaging is done over 4 points. When appropriate a further averaging is performed later if many cycles of the same amplitude have been acquired.

The hysteresis cycles are usually measured under a sequence of increasing magnetic fields, to simplify the magnetic history of the sample.

7. Experimental data.

We measured a few samples of YBCO and BISCCO. We present here in detail only the results obtained in an YBCO sample we call VAC IV.

The sample is cut from a wire with Ag matrix, which is left in place for the measurements.

The sample has an outer diameter of 0.5 mm including the Silver sheet and the YBCO core has a diameter of 0.34 mm

The sample lenght is about 4 mm

The starting material has an average grain size = $10\mu m$

The critical current densities for the newly prepared sample where: J_c = 242A/cm^2 @ 77. K and J_c = 2350. A/cm^2 @ 4.2 K.

The present measurements comes after one year of ageing of the sample and the critical current density at 4.2 K is reduced to $\sim$ 400 A/cm^2

The reduced values of the transport properties are anyway useful to us and have been chosen on purpouse to simulate at 4.2 K the behaviour usually expected at liquid Nitrogen temperature, keeping low the effects coming from thermal fluctuations in the material.

The magnetic history of the sample has been analized starting as usual from low amplitude cycles, but we present first the series of hysteresis loops obtained at higher fields. In fig. 7 you can see the close similarity of the Φ vs H we have measured with the expectation of the Bean model which is shown in fig. 8. A good agreement is found if we assume a critical current density of 180 A/cm^2 and a filling factor of 95 %.

In Fig. 9 we show four hysteresis cycles taken at lower fields. In this graph you can note that the amplitude of the cycle, and in particular the difference between the residual fluxes at $H_{ext} = 0$ on increasing and decreasing fields is not an integer multiple of the flux quantum. This can seem strange at first glance but this behaviour can be easely explained by recalling that even in very simple structures, which in a sense are the ingredients from which the granular samples

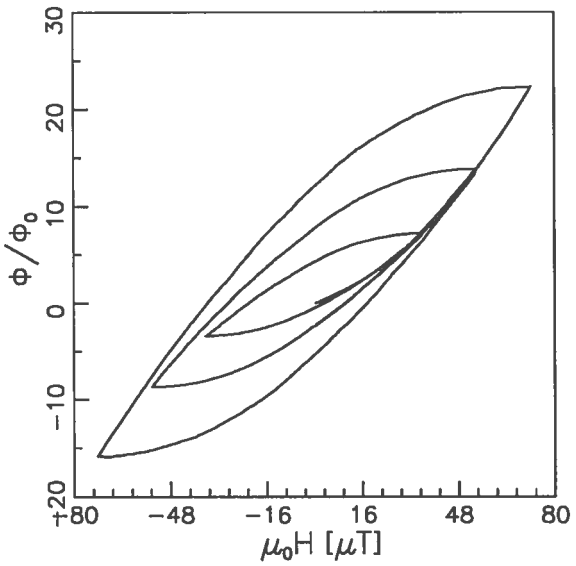

Figure 7: Three magnetization cycles at field amplitude ranging from 40 to 75 μT.

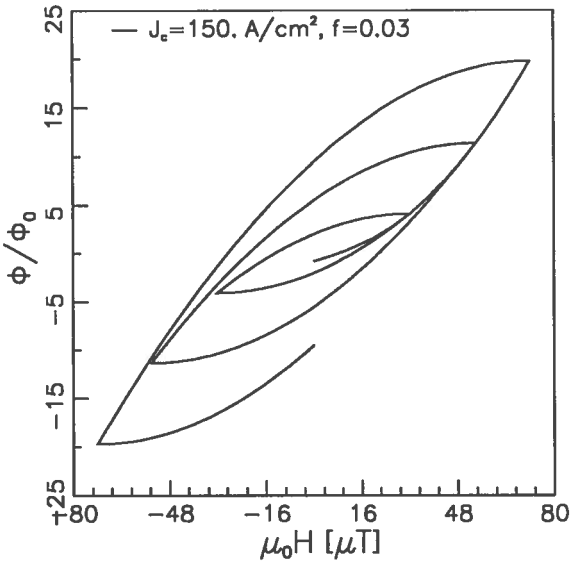

Figure 8: Magnetization cycles obtained by the Bean model.

are made, like a single superconducting loop closed by a Josephson Junction or an uniform Josephson Junction, the internal flux can be nonzero and non integer at null external field. In fig. 10 we show how the internal flux at zero external field varies in a SQUID as a function of the loop area (symbols) and in an uniform Junction as a function of its lenght.

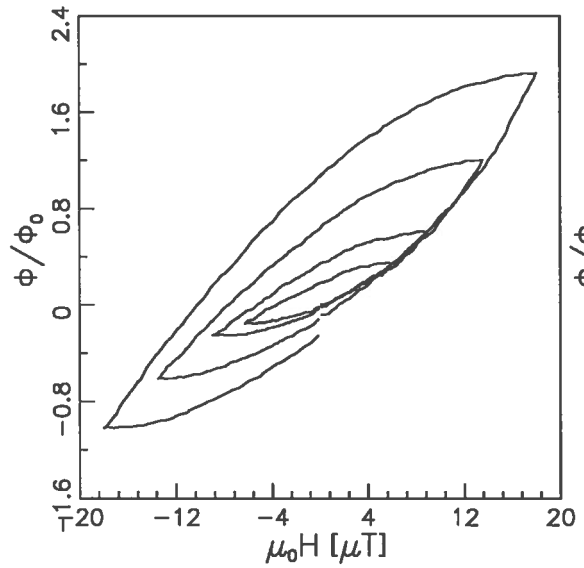

Figure 9: Hysteresis cycles measured in sample VAC IV at intermediate amplitude.

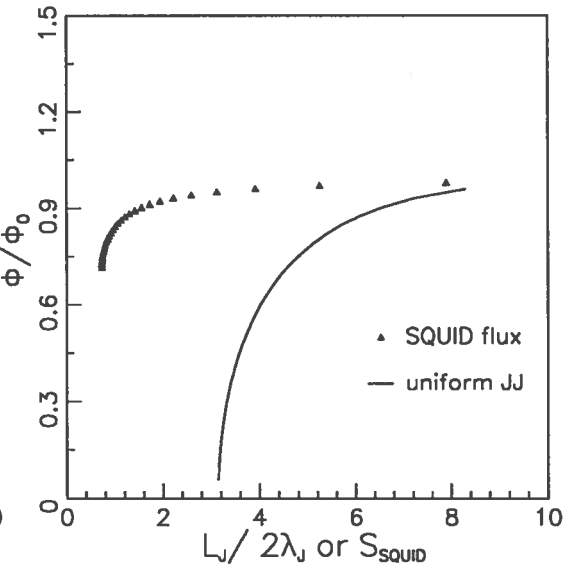

Figure 10: The internal flux in a SQUID as a function of its area (a.u.), and in an uniform Junction as a function of its relative lenght.

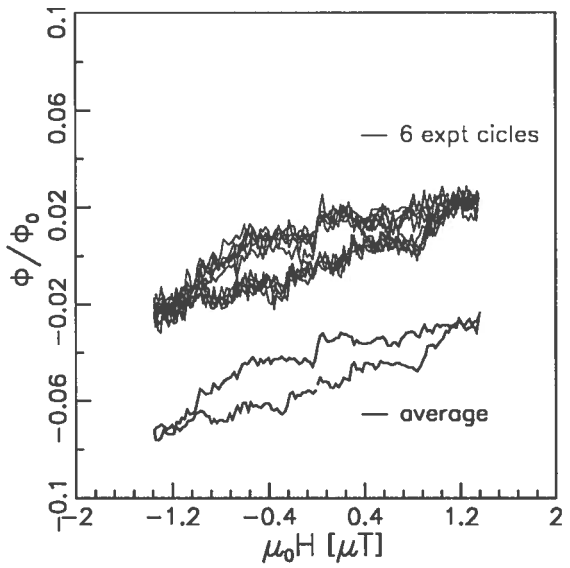

Figure 11: Six experimental cycles measured at very low field amplitude and their average.

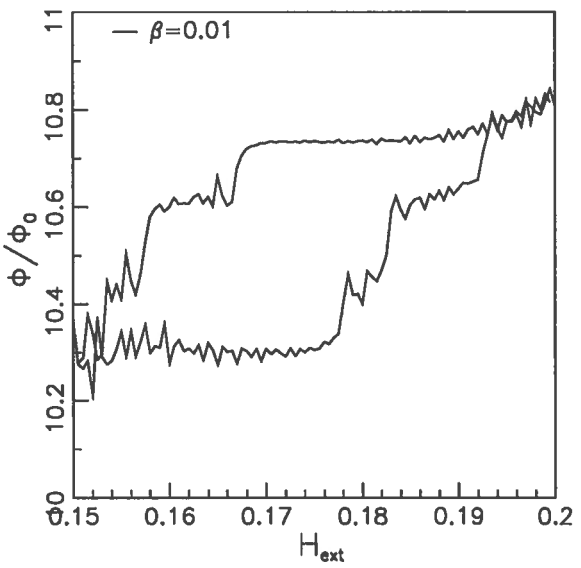

Figure 12: Non-integral flux steps in a two-dimensional simulation of a sample with $\beta/2\pi$=0.01

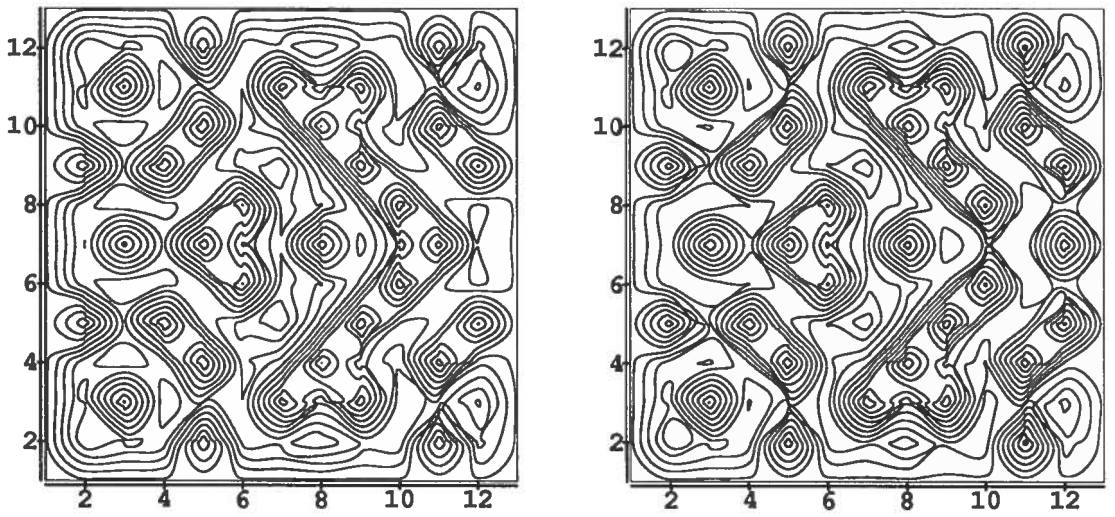

Figure 13: The magnetic field distribution in the sample at two different field levels. The fluxon on the center of the right side is moved by one mesh site.

The first cycles which show hysteresis were obtained at magnetic fields of the order of 1 μT. A sequence of six cycles measured at such a field level is shown in fig. 11. The irreversibility of the behaviour is clearly seen and is confirmed by the averaged cycle shown in the picture. The cycle presents a few steps, of which the central one is the more apparent, with a flux change of a few percent of the flux quantum.

Of course we cannot attribute such a step to the entrance of a fluxon in the sample.

We decided at this time to have a closer look at the simulation analizying a system with a $\beta/2\pi = 0.01$, performing small cycles around a nonzero external field after having trapped a few fluxons inside. The results of such a simulation are shown in fig. 12 in which flux steps of $\sim 0.1\Phi_0$ can be seen. The larger amplitude of the step compared with the experimental ones can be attributed to the fact that we use a 2-D simulation, and in this case we did not even introduced a statistical distribution.

Corresponding to this small steps the field map in the sample shows clearly the movement of the fluxons sitting near the boundary of one cell, as shown in fig. 13, which corresponds to the central flux jump in decreasing field in fig.12.

The origin of the jumps in the experimental data, in spite of their smaller size, which can be due to a partial movement in the third direction (along the field), can be explained by the same effect.

8. Conclusions

The use of a new magnetometer of very high sensitivity, tailored to the specific needs of the measurement of magnetization in superconductors at low fields, has allowed us to detect in high T_c superconducting samples the presence of fluxons and their movement from one pinning center to another.

We have shown that the pinning in granular superconductors come out directly from the discretness of the system, formed by superconducting grains connected by Josephson Junctions, while the statistical distribution of the properties of the material changes only slightly its macroscopic behaviour. The magnetic history of the sample is determined by the critical state model.

Intergranular fluxons can be spread over several cells of the network of junctions, if the junctions have low critical current, and still be pinned and follow a critical state model.

The hysteresis cycles can show at low fields, for small samples made by low current materials, quantum structures (due to individual fluxons) mixed with the usual macroscopic behaviour.

While a quantitative agreement between the experiment and our numerical model is hardly possible, because of the simplified treatment, based on a 2-D model with pointlike junctions, qualitavely we were able to explain all the features seen experimentally.

References

1. P. Chaudhari, J. Mannhart, D. Dimos, C. C. Tsuei, J. Chi, M. M. Oprysko and M. Scheurmann, *Phys. Rev. Lett.* **60** (1988) 1653
2. V. Calzona, M.R. Cimberle, C. Ferdeghini, F. Pupella, M. Putti, C. Rizzuto, A. Siri and R. Vaccarone, *Cryogenics* **30** (1990) 569
3. C. P. Bean, *Rev. Mod. Phys.* **36** (1964) 31
4. R. Vaccarone, *Proc. 3rd National Meeting on High Temperature Superconductivity*, Feb. 12-14, 1990, Genoa, Italy, p. 346
5. T. Yamashita and L. Rinderer, *J. Low Temp. Phys.* **21** (1975) 153
6. A. Giannelli and C. Giovannella, *Proc. 3rd National Meeting on High Temperature Superconductivity*, Feb. 12-14, 1990, Genoa, Italy, p. 358
7. C. J. Lobb, D. W. Abraham and M. Tinkham, *Phys. Rev. B* **27** (1983) 150
8. F. Parodi and R. Vaccarone, *Phisica C* **173** (1991) 56